

**PHASES OF MIRROR SYMMETRY**

TI-MING CHIANG and BRIAN R. GREENE<sup>†</sup>

*F.R. Newman Lab. of Nuclear Studies, Cornell University  
Ithaca, NY 14853, USA*

**Abstract**

We review the geometrical framework required for understanding the moduli space of  $(2, 2)$  superconformal-field theories, highlighting various aspects of its phase structure. In particular, we indicate the types of phase diagrams that emerge for “generic” Calabi-Yau theories and review an efficient method for their determination. We then focus on some special types of phase diagrams that have bearing on the issues of rigid manifolds, mirror symmetry and geometrical duality.

**1. Introduction**

In the last few years a tremendous amount of progress has been made in understanding the structure of  $N = 2$  conformal field theory moduli space. Most impressive has been the emergence of a rich phase structure [1] [2] for those theories that can be realized as the infrared limit of  $N = 2$  two dimensional gauged linear sigma models [1]. Amongst such theories, for the case of abelian gauge groups, are nonlinear sigma models on Calabi-Yau target spaces and Landau-Ginzburg theories. The phase structure describing these theories has led both to interesting new physics, such as spacetime topology change [1] [2], as well as clarified some previously puzzling features of mirror symmetry. Examples of the latter include the precise statement of the relationship between the Kähler moduli space of a Calabi-Yau space and the complex structure moduli space of its mirror (which is closely related to the results on spacetime topology change) as well as the resolution of how mirror symmetry applies to rigid Calabi-Yau manifolds (whose putative mirror would appear to lack a Kähler form).

In the present talk we will briefly review the phase picture of  $N = 2$  moduli space, discuss its application to “generic” examples, and then illustrate its utility in discussing “non-generic” examples. Among the generic examples we illustrate the tremendous growth rate of the number of phases with increasing  $h^{1,1}$ . For instance, we note an example with more than 700,000 phases. Among the nongeneric examples are cases in which there’s no Calabi-Yau sigma model phase, no Landau-Ginzburg phase, or *all* Calabi-Yau sigma model phases. We discuss these examples

---

<sup>†</sup> Talk delivered by B.R.G at the *Strings '95* conference, March 13-18, 1995, USC.

with particular reference to the issues of mirrors of rigid manifolds and geometrical  $R \leftrightarrow 1/R$  type duality.

## 2. The Phase Picture

The phase picture of  $N = 2$  conformal field theory moduli space was arrived at by two independent lines of investigation [1] [2]. The former sought to provide a more robust argument relating Calabi-Yau sigma models to Landau-Ginzburg theories than provided in [3] while the latter sought to resolve a troubling issue in mirror symmetry. When the dust settles, the two analyses yield the same result: the classical Kähler moduli space of a Calabi-Yau sigma model is but a subset of the corresponding quantum conformal field theory moduli space. The latter “enlarged Kähler moduli space” consists of numerous regions glued along common boundaries with the natural identity of the corresponding physical model changing from region to region. By natural identity we mean the formulation of the model for which perturbation theory is reliable. In the simplest examples of one dimensional moduli spaces there are two regions – typically consisting of a Calabi-Yau sigma model region and a Landau-Ginzburg region. Examples with higher dimensional moduli spaces can have a far richer phase structure.

We first review the phase structure of these moduli spaces from the viewpoint of [2] and subsequently return to the approach of [1] by establishing a dictionary between these two approaches, as discussed in [4].

The problem which motivated the work in [2] is simple to state: according to mirror symmetry if  $M$  and  $W$  are a mirror pair, then the complex structure moduli space of  $M$  isomorphic to the (complexified) Kähler moduli space of  $W$  and vice versa; mathematically, though, they appear to be anything but isomorphic. This problem is most easily understood by directly comparing the typical form of a complexified Kähler moduli space with that of a complex structure moduli space.

### 2.1 Kähler Moduli Space

Classically, the Kähler form on a Calabi-Yau space is a closed two form  $J$  related to the metric  $g$  via

$$J = ig_{i\bar{j}}dX^i \wedge dX^{\bar{j}}. \tag{1}$$

As such,  $J$  may be thought of as an element of the vector space of all closed two forms (modulo exact forms)  $H^2(M, \mathbb{R})$ . In fact,  $J$  lies in a special subspace of this vector space known as the Kähler cone by virtue of its relation to the metric. In particular, since the metric measures non-negative lengths, areas and volumes,  $J$

satisfies

$$\int_M J \wedge J \wedge J > 0 \tag{2}$$

$$\int_S J \wedge J > 0 \tag{3}$$

$$\int_C J > 0. \tag{4}$$

where  $S$  and  $C$  are nontrivial 4 and 2-cycles on the manifold respectively.

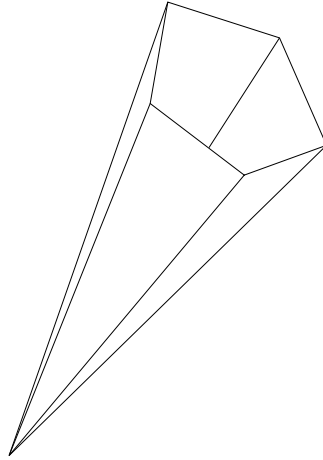


Figure 1a. Schematic diagram of Kähler cone.

The space of all  $J$  in  $H^2(M, \mathbb{R})$  that satisfy these requirements has a cone structure because if  $J$  satisfies these conditions, so does the positive ray generated by  $J$  – hence the name Kähler cone. In figure 1a we schematically show a Kähler cone. A well known aspect of string theory is that it instructs us to combine the Kähler form  $J$  with the antisymmetric tensor field  $B$  into the complexified Kähler class  $K = B + iJ$ . The physical model is invariant under integral shifts of  $B$  (more precisely, shifts of  $B$  by elements of  $H^2(M, \mathbb{Z})$ ) which motivates changing variables to

$$w_l = e^{2\pi i(B_l + iJ_l)} \tag{5}$$

where  $(B_l, J_l)$  are coefficients in the expansion of  $B$  and  $J$  with respect to an integral basis of  $H^2(M, \mathbb{Z})$ . These new variables have the invariance under integral shifts built in.

The imaginary part of  $K$  satisfies the conditions on  $J$  just discussed and hence the Kähler cone of figure 1a becomes the bounded domain of  $H^2(M, \mathbb{C})$  in the  $w$  variables as depicted in figure 1b. We note that the boundary of this region denotes

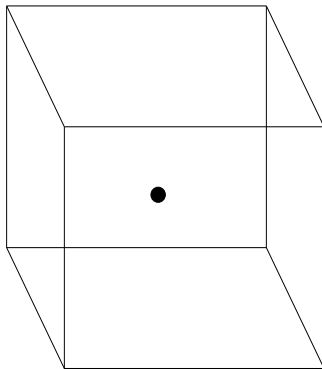


Figure 1b. Complexified Kahler cone.

those places in the parameter space where the Kähler form  $J$  degenerates in the sense that some of the positivity requirements are violated.

We will return to this picture shortly, but first we turn to a discussion of the typical form of complex structure moduli spaces.

## 2.2. Complex Structure Moduli Space

Mathematically, the choice of complex structure on a manifold is the choice of local complex coordinates in sets of coordinate patches and holomorphic transition functions between patches.<sup>1</sup> Physically, just as the choice of Kähler class determines the metric or “size” of the Calabi-Yau space, the choice of complex structure determines its “shape”. For instance, in the simplest case of a Calabi-Yau manifold, the one-complex dimensional torus, the Kähler structure fixes the overall volume while the complex structure fixes  $\tau$ , the angle between the two cycles.

The typical form of Calabi-Yau spaces we shall consider is given by the vanishing locus of homogeneous polynomial equations in (products of) projective spaces. For ease of discussion, consider the case of a single equation  $P = 0$  with

$$P = \sum a_{i_1 \dots i_n} z_1^{i_1} \dots z_n^{i_n}. \quad (6)$$

It is known that by varying the coefficients in such equations we vary the choice of complex structure on the the Calabi-Yau space. There is one constraint on the choice of coefficients  $a$  which we must satisfy: they must be chosen so that  $P$  and its partial derivatives do not have a common zero in the defining projective space. If they did have such a common zero, the choice of complex structure would be singular

---

<sup>1</sup>These choices are equivalent if they differ by a biholomorphic change of variables.

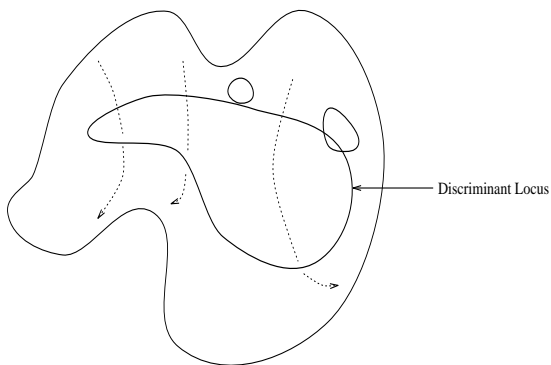


Figure 2. Complex structure moduli space showing discriminant locus.

(non-transverse). It is straightforward to see that this places one complex constraint on the choice of coefficients and hence we can think of the complex structure moduli space as the space of all  $a$ 's (modulo those which are equivalent via coordinate transformations on the  $z$ 's) less this one complex constraint. Schematically, this space can be illustrated as in figure 2 where the “bad” choice of  $a$ 's is correctly denoted as the *discriminant locus*<sup>2</sup>.

### 2.3. The Problem

The puzzle for mirror symmetry can now be described directly. Mirror symmetry tells us that figure 1b and figure 2 are isomorphic if the former is for  $M$  and the latter for its mirror  $W$ . However, manifestly they are not. This is not a product of our schematic drawings as there are genuine qualitative distinctions. Most prominently, note that the locus of what *appear* to be badly behaved theories is real codimension one in the Kähler parameter space, occurring on the walls of the domain where the classical Kähler form degenerates. On the contrary, the locus of badly behaved theories in the complex structure moduli space, as just discussed, is real codimension two (complex codimension one). What is going on? The answer to this question was found in [1] and [2] and implies that:

- 1: Figure 1b for  $M$  is only a *subset* of figure 2 for  $W$ . To be isomorphic to figure 2 of  $W$ , it must be augmented by numerous other regions, of a similar structure, all

---

<sup>2</sup>Recently, it has been shown that at least some and possibly all points on the discriminant locus correspond to well defined string theories with the singularities in the conformal field theory description associated with the appearance of new massless degrees of freedom [5] [6] . We will not discuss this issue here.

adjoined along common walls. This yields the *enlarged Kähler moduli space* of  $M$ .

- 2: Some of these additional regions are interpretable as the complexified Kähler moduli space of *flops* of  $M$  along rational curves. These are relatively subtle transformations of one Calabi-Yau manifold to yield other (birationally equivalent) possibly topologically distinct Calabi-Yau's.

- 3: Other regions may not have a direct sigma model interpretation, but rather are the parameter spaces for Landau-Ginzburg theory, Calabi-Yau orbifolds, and various relatively unfamiliar hybrid combination conformal theories.

- 4: Whereas classical reasoning suggests that theories whose complexified Kähler class lies on the wall of a domain such as that in figure 1b are ill defined, quantum reasoning shows that the generic point on such a wall corresponds to a perfectly well behaved theory. Thus, physics changes *smoothly* if the parameters of a model change in a generic manner from one region to another by crossing through such a wall. As some such regions correspond to sigma models on topologically distinct target spaces, this last point establishes the first concrete example of physically allowed spacetime topology change.

We can pictorially summarize this discussion as we do in figure 3. Here we see that the abstract conformal field theory moduli space is geometrically interpretable in terms of the complex structure and enlarged Kähler structure parameter spaces associated to  $M$  or to the enlarged Kähler structure and complex structure parameter spaces associated to the mirror  $W$ . This picture allows us to elaborate on point 4 above. Let's imagine following a path in the enlarged Kähler moduli space of  $M$  that passes through a wall between two sigma model regions. As mentioned, at first sight it appears that the corresponding sigma model is ill defined when the parameters are those associated with the wall since the Kähler form has degenerated. Examining the quantum theory directly, we see that the question as to whether or not it is well behaved is hard to answer since reliable perturbation theory requires that distances be suitably large (recall that the expansion parameter is  $\frac{\alpha'}{R^2}$ ) while certain lengths shrink to zero on the wall. Thus, probing the physical meaning of passing through a wall by direct analysis does not yield a definitive conclusion. Now, though, mirror symmetry comes to the rescue. We can rephrase the journey taken in the Kähler moduli space of  $M$  as a journey in the complex structure moduli space of  $W$ . Furthermore, nothing in our discussion has dealt with the complex structure of  $M$ , so we can choose it at our convenience (and keep it fixed throughout the analysis). We choose it so that the corresponding mirror Kähler structure in the enlarged Kähler moduli space of  $W$  is far from any walls and hence deeply in the perturbative realm. In this way, the *strong* coupling question of analyzing the physics of passing through a wall in the  $M$  description has been translated into a

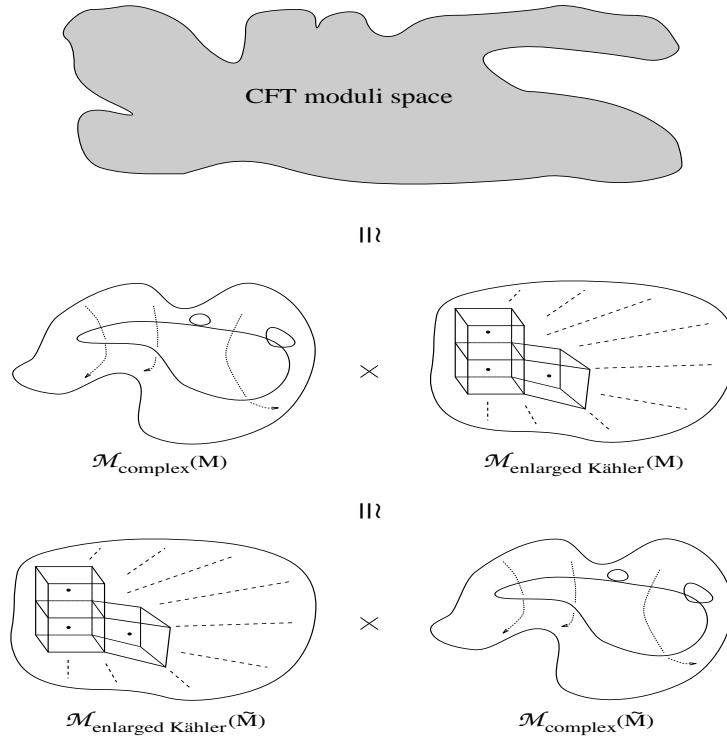


Figure 3. Schematic drawing of the moduli spaces for  $M$  and it's mirror  $W$

*weak* coupling question on  $W$ . Now, a journey through the complex structure moduli space of  $W$ , keeping the Kähler structure fixed at a value ensuring perturbative reliability, yields perfectly well behaved physics so long as we stay away from the discriminant locus. As the latter is real codimension two, this is simple to do: the generic path misses the bad theories. Since we trust this analysis, the same must be true for the physically isomorphic mirror path on  $M$  and hence physics is smooth as we pass through a generic point on a Kähler wall.

### 3. Constructing the Phase Diagram

The works of [1] and of [2] present two different methods for constructing the phase diagram for any given example. Each has its virtues so lets briefly review them both.

#### 3.1. Toric Geometry: Symplectic Quotients

In [1], Witten starts with a gauged linear sigma model in two dimensions and studies its vacuum structure for various values of coefficients of Fayet-Illiopoulos

D-terms. To be concrete, consider the case of the quintic hypersurface which corresponds to gauge group  $U(1)$ . The field content of this theory consists of six chiral superfields  $P, \Phi_1, \dots, \Phi_5$  with charges  $(-5, 1, 1, 1, 1, 1)$ . From these fields we can build a gauge invariant superpotential  $PG(\Phi_1, \dots, \Phi_5)$  where  $G$  is a transverse quintic polynomial in the  $\Phi$ 's. The detailed form of the Lagrangian can be found in [1]; for our purpose we shall only be concerned with the bosonic potential which takes the form

$$U = |G|^2 + |p|^2 \left( \sum \left| \frac{\partial G}{\partial \phi_i} \right|^2 \right) + \left( \sum |\phi_i|^2 - 5|p|^2 - r \right)^2 \quad (7)$$

where  $r$  is the coefficient of the D-term and we have dropped terms that will not play a direct role in our discussion.

We now study the vacuum structure for various choices of  $r$ . In fact, qualitatively there are only two distinct cases:  $r$  positive and  $r$  negative. We consider each in turn. When  $r$  is positive we learn that not all of the  $\phi_i$  can vanish simultaneously. By the transversality of  $G$  we then learn that  $p$  must vanish. Thus, the vacuum is given by  $G = 0$  inside of  $\sum |\phi_i|^2 = r$ . In fact, since we are dealing with a  $U(1)$  gauge theory we have the further identification

$$(\phi_1, \dots, \phi_5) \equiv (e^{i\theta} \phi_1, \dots, e^{i\theta} \phi_5) \quad (8)$$

Now it is straightforward to see that the  $\phi_i$  span  $\mathbb{C}\mathbb{P}^4$ . The usual identification

$$(\phi_1, \dots, \phi_5) \equiv (\lambda \phi_1, \dots, \lambda \phi_5) \quad (9)$$

for arbitrary nonzero complex parameter  $\lambda$  is here realized in two steps: we pick out one point in the equivalence class by first imposing  $\sum |\phi_i|^2 = r$ , which determines the magnitude of  $\lambda$  and then by imposing (8) which eliminates the remaining phase ambiguity. Thus, for  $r$  positive the vacuum state is the vanishing of the quintic  $G$  in  $\mathbb{C}\mathbb{P}^4$ , the most well known Calabi-Yau manifold.

For  $r$  negative we proceed in a like fashion. We immediately find that  $p$  can not be zero and that all of the  $\phi_i$  must vanish. Using the gauge freedom to fix the phase of  $p$  we thus learn that we have massless fluctuating modes about a unique vacuum state – in other words a Landau-Ginzburg model. Thus we see that this linear sigma model effectively has two phases: a Calabi-Yau sigma model phase and a Landau-Ginzburg phase. Three points of clarification are called for.

- 1: The parameter  $r$  is actually the real part of a complex parameter  $t$  (whose imaginary part is a theta angle). Thus each phase is actually two real dimensions meeting along a common one dimensional locus. After suitable compactification, we can think of these two regions as the northern and southern hemispheres meeting

along the equator. As argued by Witten, the conformal field theory is well behaved so long as  $\theta$  is not zero, and hence there is no obstruction to passing from one phase to another.

- 2: It is worthwhile to think about the D-term part of the vacuum analysis just described as separate from the full bosonic potential discussion. For  $r$  positive the space is  $(\phi_1, \dots, \phi_5; p)$  with not all  $\phi_i$  zero simultaneously subject to the (gauge) equivalence relation

$$(\phi_1, \dots, \phi_5; p) \equiv (\lambda\phi_1, \dots, \lambda\phi_5; \lambda^{-5}p). \quad (10)$$

This space is recognized as the line bundle  $\mathcal{O}(-5)$  over  $\mathbb{C}\mathbb{P}^4$ . For  $r$  negative, since  $p$  is nonzero, we can solve the equivalence relation by setting  $p$  to one, modulo a left over  $\mathbb{Z}_5$  ambiguity. Thus, the space of fields is  $\mathbb{C}^5/\mathbb{Z}_5$ . Mathematically, the line bundle  $\mathcal{O}(-5)$  over  $\mathbb{C}\mathbb{P}^4$  and  $\mathbb{C}^5/\mathbb{Z}_5$  are very closely related: they are birationally equivalent. This simply means that they agree except on lower dimensional subspaces. One can see this by recalling that the blow up of the origin in  $\mathbb{C}^5/\mathbb{Z}_5$  is the line bundle  $\mathcal{O}(-5)$  over  $\mathbb{C}\mathbb{P}^4$ . Thus, away from this exceptional set, they agree. The interpolation from one phase to another is thus seen as a particular kind of birational transformation on the embedding space. In fact, setting the D-term  $(\sum |\phi_i|^2 - 5|p|^2 - r)$  to zero is, mathematically speaking, known as setting a *moment map* to zero. Combining this with the  $U(1)$  gauge equivalence is known as performing a symplectic quotient. The resulting ambient spaces are *toric varieties* realized via symplectic quotients.

- 3: For ease of discussion we have focused on the case in which the Kähler moduli space is one dimensional, i.e. a single  $U(1)$  gauge group. More generally, this number can be larger (or smaller, as we shall discuss shortly) yielding a much richer phase structure. For instance, if the enlarged Kähler moduli space is  $n$  dimensional, we will have a  $U(1)^n$  gauge group and parameters  $(r_1, \dots, r_n)$  multiplying the respective Fayet-Illiopoulos D-terms. In fact, in many examples there are different phase regions corresponding to nonlinear sigma models on topologically distinct Calabi-Yau target spaces. The ability to freely move from one phase region to another in such examples gives rise to physically smooth topology changing processes.

### 3.2. Toric geometry: Holomorphic quotients

The symplectic approach to building the embedding space of our models is directly transcribable, as we have seen, into the language of Lagrangian dynamics. The equivalent holomorphic approach is somewhat more removed from the physical description, but is often more powerful for understanding the phase structure.

The mathematical ideas are quite simple. Consider  $\mathbb{P}^n$  realized as  $\frac{\mathbb{C}^{n+1} - (0, \dots, 0)}{\mathbb{C}^*}$ . This is the simplest example of a toric variety realized as a holomorphic quotient: we start with  $\mathbb{C}^{n+1}$ , remove some set of lower dimension (in this case just the origin) and holomorphically divide by  $\mathbb{C}^*$ . This immediately yields a natural generalization: start with  $\mathbb{C}^{n+1}$ , remove some set that we shall call  $F_\Delta$  and holomorphically divide by  $(\mathbb{C}^*)^m$ . Two such toric varieties which differ only by the set  $F_\Delta$  which is removed are birationally equivalent (as clearly they agree everywhere except on a set of lower measure).

Lets consider the example discussed in the previous subsection, now in the holomorphic language. Begin with  $\mathbb{C}^6$  with six complex “coordinates”  $(\phi_1, \dots, \phi_5; p)$ . On this space define a  $\mathbb{C}^*$  action

$$(\phi_1, \dots, \phi_5; p) \rightarrow (\lambda\phi_1, \dots, \lambda\phi_5; \lambda^{-5}p). \quad (11)$$

Let  $F_{\Delta_1}$  be  $(0, \dots, 0; p)$  and  $F_{\Delta_2}$  be  $(\phi_1, \dots, \phi_5; 0)$ . The first choice yields  $\mathcal{O}(-5)$  over  $\mathbb{C}\mathbb{P}^4$  and the second yields  $\mathbb{C}^5/\mathbb{Z}_5$ .

The important point for our purpose here is that the holomorphic approach gives a simple combinatorial method for working out the phase diagram of any example as we now briefly describe. The different phase regions of a given example constitute a particular class of birational transformations on any “seed” member of the phase structure. In the holomorphic approach, these different birational models are specified by different choices for the set  $F_\Delta$ . The set of allowed choices for the  $F_\Delta$  are in one to one correspondence with the set of triangulations of a particular point set in  $\mathbb{R}^n$  for an n-dimensional toric variety. We will not discuss this point set in detail here, as it is fully discussed in [2] and in [4]. Our point is simply to emphasize that whereas in the symplectic approach one needs to find regions in the parameter space of  $(r_1, \dots, r_n)$  corresponding to the same vacuum state of the linear sigma model, in the holomorphic approach one only needs to find the set of distinct triangulations of a point set in  $\mathbb{R}^n$ .

Just to give a feel for how this goes in a simple example, lets again return to the case of the quintic. Consider the point set

$$\begin{aligned} \alpha_1 &= (1, 0, 0, 0, 1) \\ \alpha_2 &= (0, 1, 0, 0, 1) \\ \alpha_3 &= (0, 0, 1, 0, 1) \\ \alpha_4 &= (0, 0, 0, 1, 1) \\ \alpha_5 &= (-1, -1, -1, -1, 1) \\ \alpha_6 &= (0, 0, 0, 0, 1) \end{aligned}$$

in  $\mathbb{R}^5$ . (To understand why this is the relevant point set to consider, consult [2].) The algorithm for finding the possible  $F_\Delta$  requires that we find the possible triangulations of this point set. There are two: The first corresponds to the Calabi-Yau phase and is given by the union of 5 cones, each of which contains 4 points chosen from the set  $\{\alpha_1, \alpha_2, \alpha_3, \alpha_4, \alpha_5\}$  and  $\alpha_6$ , and the second gives the Landau-Ginzburg phase with only one cone  $\{\alpha_1, \alpha_2, \alpha_3, \alpha_4, \alpha_5\}$ .

A lower dimensional version of this, as given in the figure, may help with visualization. In this figure, the central point on the top face denotes  $\alpha_6$  and we see that the two triangulations differ by whether or not this point is included. The lowest point represents the origin of the space.

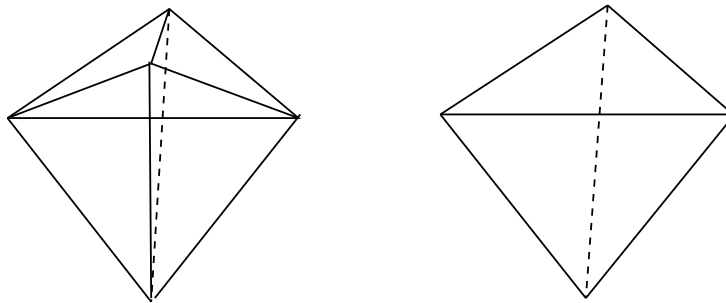


Figure 4. The Calabi-Yau and Landau-Ginzburg phase for the quintic.

Now, to each triangulation, as discussed in [2], we find the point set  $F_\Delta$  according to

$$\bigcap_{\sigma \in \Delta} \left\{ x \in \mathbb{C}^6; \prod_{\alpha_i \notin \sigma} x_i = 0 \right\} \quad (12)$$

where  $\sigma$  denotes a cone in the fan  $\Delta$ .

We see that this formula, applied to the two triangulations, does in fact yield the two point sets discussed above.

One feature that we have not mentioned is how, in examples with more than two phase regions in a higher dimensional setting, we glue the various phase regions together. There is also a simple combinatorial way of doing this as discussed in [2], but for lack of time we shall not go into that here.

### 3.3. Generalization:

In our discussion so far we have implicitly assumed that we start with some Calabi-Yau manifold embedded in some toric variety such as a weighted projective

space or products thereof. We can then fill out the full phase diagram, of which this Calabi-Yau description is but one member, by using either the symplectic or holomorphic formalism described above. In the former, we realize the toric embedding space via a gauged linear sigma model, and then determine the form of all possible vacuum states by varying the Fayet-Illiopoulos D-terms. In the latter we realize the embedding space in the formalism of toric geometry and then determine all Kähler birational transformations via a combinatorial procedure. Given such a phase diagram, no one region is any more special than any other and hence one might suspect that one need not start out from a Calabi-Yau manifold in a toric variety. Rather, in the symplectic formalism we may start with any linear sigma model with the requisite nonanomalous R-symmetries that flow in the infrared to the  $U(1)$  currents in the  $N = 2$  superconformal algebra. In the holomorphic formalism, we can start with any toric point set data with suitably mild singularities that, again, gives rise in the corresponding physical model to the necessary nonanomalous R-symmetries. Technically, such toric data corresponds to that for *reflexive Gorenstein cones* [7].<sup>3</sup> Given such data, in either formalism, one can then build the phase diagram, in the manner outlined above. An important fact is that, for a general example, nothing guarantees that the phase diagram will contain a Calabi-Yau sigma model region or even a Landau-Ginzburg region. The fact that there may not be a Landau-Ginzburg region was explicitly shown in some of the examples in [1] in which, for instance, the closest cousin to a Landau-Ginzburg theory is a gauged Landau-Ginzburg theory. Below we shall see some examples that lack a Calabi-Yau sigma model region.

Our program for building phase diagrams, using the holomorphic formalism, is thus clear:

- 1. Select a point set corresponding to a reflexive Gorenstein cone.
- 2. Find all possible (regular) triangulations.
- 3. Using these triangulations, build the phase diagram and establish the physical identity of each phase.

We now present the results of such a program.

#### 4. Generic Examples of Phase Diagrams

In the first class of examples, we start with toric data used to describe (complete intersection) Calabi-Yau manifolds in (products of weighted) projective space(s). Thus, in these examples, we are guaranteed to have a Calabi-Yau sigma model region. Below we present a number of examples, of increasing Kähler moduli space dimension, to illustrate the type of phase diagrams which arise.

---

<sup>3</sup>For more details in language geared to physicists see [4].

We start first with a degree-18 hypersurface in the weighted projective space  $\mathbb{P}_{(6,6,3,2,1)}^4$ . It has a  $h^{1,1} = 7$  and  $h^{2,1} = 79$ . As discussed in [2], only a 5-dimensional subspace of the  $(1,1)$ -forms on the manifold is realized torically. The point set describing the toric variety is

$$\begin{aligned} \alpha_1 &= (-3, -3, -1, -1, 1) \\ \alpha_2 &= (-2, -2, -1, 0, 1) \\ \alpha_3 &= (-4, -4, -2, -1, 1) \\ \alpha_4 &= (-1, -1, 0, 0, 1) \\ \alpha_5 &= (1, 0, 0, 0, 1) \\ \alpha_6 &= (0, 1, 0, 0, 1) \\ \alpha_7 &= (0, 0, 1, 0, 1) \\ \alpha_8 &= (0, 0, 0, 1, 1) \\ \alpha_9 &= (-6, -6, -3, -2, 1) \end{aligned}$$

The 100 triangulations of this set [2] contains 5 Calabi-Yau resolutions which can be specified by looking at the face spanned by  $\{\alpha_7, \alpha_8, \alpha_9\}$ , depicted in figure 5.

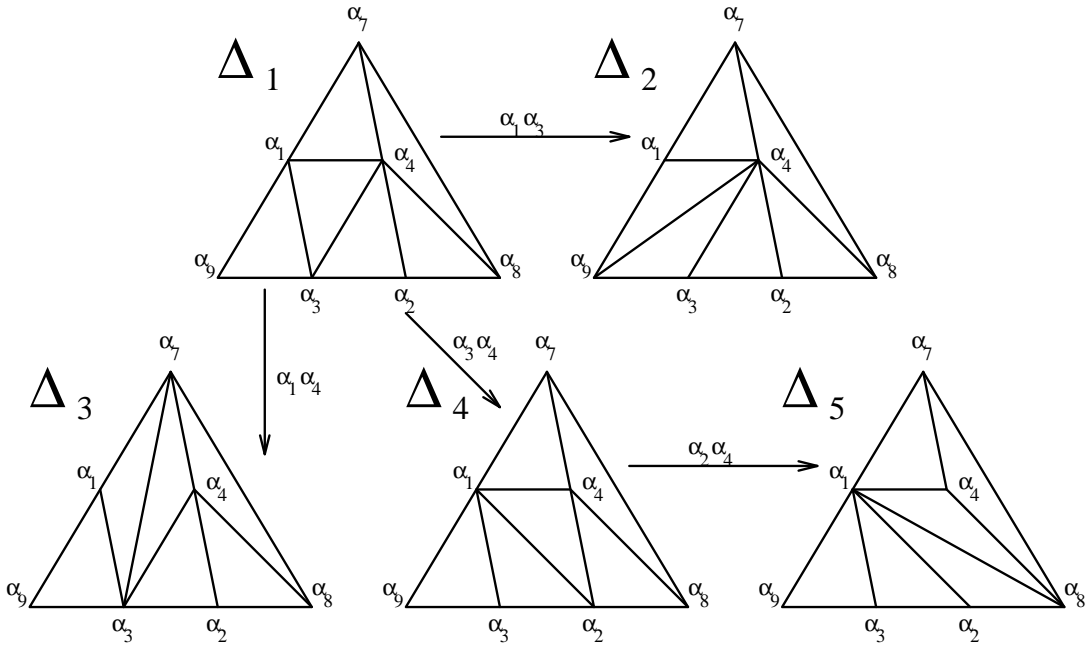


Figure 5. The 5 smooth resolutions for  $\mathbb{P}_{6,6,3,2,1}^4$

Besides the 5 Calabi-Yau regions, there is the obvious Landau-Ginzburg region comprised of the single simplex  $\{\alpha_5, \alpha_6, \alpha_7, \alpha_8, \alpha_9\}$  having volume 18. Then there are 27 Calabi-Yau orbifolds obtained by special star *unsubdivisions* of the Calabi-Yau phases we had, that is, by removing an interior point from a phase that gives us a new triangulation with all simplices still having the origin  $(0, 0, 0, 0, 1)$ . This gives rise to  $\mathbb{Z}_2, \mathbb{Z}_3, \mathbb{Z}_2 \times \mathbb{Z}_2, \mathbb{Z}_4$  and  $\mathbb{Z}_6$  quotient singularities. The remaining 67 triangulations correspond to Landau-Ginzburg *hybrid models*.

We may build the *secondary fan* which describes the moduli space of the phases using a technique described in [2]. In figure 6 we depict the connectivity of the phases in the above example by plotting vertices chosen from the interior of each separate phase.

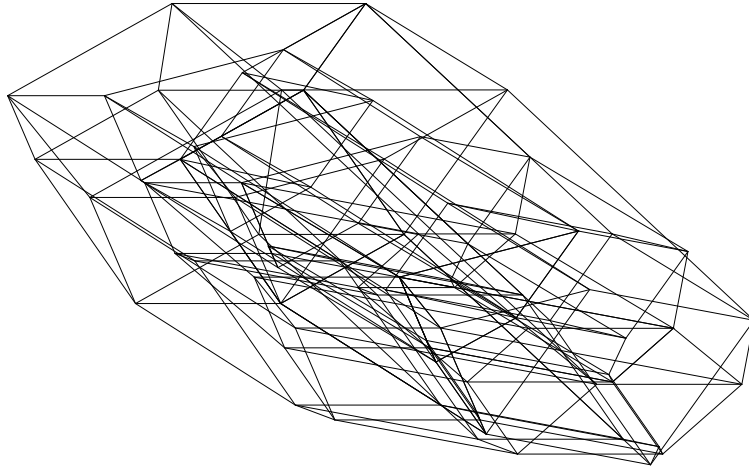


Figure 6. The connectivity of the 100 phases of  $\mathbb{P}_{6,6,3,2,1}^4$

Now we'll turn to examples involving CICYs (Calabi-Yau complete-intersections) in products of ordinary projective spaces. A CICY (more precisely a family of CICYs) is described by a configuration matrix:

$$\left( \begin{array}{c|cccc} n_1 & a_{11} & a_{12} & \dots & a_{1k} \\ n_2 & a_{21} & a_{22} & \dots & a_{2k} \\ \vdots & \vdots & \vdots & \ddots & \vdots \\ n_r & a_{r1} & a_{r2} & \dots & a_{rk} \end{array} \right) \quad (13)$$

Here  $n_i$  is a shorthand for  $\mathbb{P}^{n_i}$  and the  $a'_{ij}$ s are interpreted as degrees of  $k$

polynomials which intersect transversely, the  $j^{\text{th}}$  of which is homogenous of degree  $a_{ij}$  in the variables of  $\mathbb{P}^{n_i}$ .

In the phases picture we may formulate the problem as follows. Let us associate to the  $i^{\text{th}}$  projective space the chiral superfields  $\phi_{il}$  where  $l$  runs from 1 to  $n_i + 1$ . We will be considering a  $U(1)^r$  gauged linear sigma model based on the  $\phi$ 's as well as  $k$  other chiral superfields  $p_j$  representing the constraints.  $p_j$  will have charge  $-a_{ij}$  under the  $i^{\text{th}}$   $U(1)$ . Thus we may form the gauge-invariant superpotential

$$W = \sum_{i=1}^k p_i G_i(\{\phi_{jk}\}) \quad (14)$$

where  $G_i$  is the  $i^{\text{th}}$  constraint and the bosonic potential has the following form:

$$U = \sum_{i=1}^k \left| \frac{\partial W}{\partial p_i} \right|^2 + \sum_{i=1}^r \sum_{j=1}^{n_i+1} \left| \frac{\partial W}{\partial \phi_{ij}} \right|^2 + \sum_{i=1}^r \left( \sum_{j=1}^{n_i+1} |\phi_{ij}|^2 - \sum_{j=1}^k a_{ij} |p_j|^2 - r_i \right)^2 \quad (15)$$

Transversality of the  $G_i$ 's imply that the conditions necessary for the minimization of the potential:

$$\frac{\partial W}{\partial p_1} = \dots = \frac{\partial W}{\partial p_k} = \frac{\partial W}{\partial \phi_{11}} = \dots = \frac{\partial W}{\partial \phi_{rn_r+1}} = 0 \quad (16)$$

are realized if and only if the set of fields  $p_i$  all vanish or the  $\phi_{ij}$ 's vanish for some  $i$ .

Again, one could work out the phase diagram by studying the semi-classical vacua for various choices of the  $r$  parameters and grouping together those which yield the same phase. We follow the holomorphic approach by realizing the ambient toric variety (which here is just a product of ordinary projective spaces) as the associated point set and then seeking out all possible triangulations. It is worth noting two things. First, distinct phases in the ambient toric variety may not correspond to identical phases in the actual physical model. From the toric view this is simply the statement that the Calabi-Yau is of finite codimension in the toric variety and hence may not intersect the distinct  $F_\Delta$ 's which distinguish two phases. Physically, the vanishing of the F-terms may not intersect the point set distinguishing between the vanishing locus of distinct D-terms (which differ by the  $r$ 's lying in different phase regions). Second, a given Calabi-Yau manifold can often be realized as embedded in distinct ambient toric varieties. It turns out that moduli having a toric representation in one embedding may not have a toric representation in another and vice versa. Thus, different embeddings, although yielding topologically identical Calabi-Yau's can provide different moduli space information.

In the following we show a few examples of hypersurfaces and CICYs and the total number of triangulations as well as (in the case of CICYs) the number of smooth phases<sup>4</sup>. The examples chosen illustrate a dramatic increasing trend of the number of phases with the value of  $h_{toric}^{1,1}$ . We have actually been rather selective in our presentation for the CICYs. The collection of results for about 8000 configurations with  $h_{toric}^{1,1}$  ranging from 1 to 8 show that one can find a large range in the number of phases for any  $r$  and these ranges do intersect widely. It remains true that the maximum number of phases (or smooth phases) found increases with  $h_{toric}^{1,1}$ . It is interesting to note that the  $h_{toric}^{1,1} = 6$  example shown on the next page has all of its phases being smooth. We'll say more about this in the next section.

In the following we give some examples of the number of phases found for hypersurfaces in various weighted projective spaces with 5 weights:

Manifold	$h^{1,1}$	$h^{2,1}$	$h_{toric}^{1,1}$	Phases
$\mathbb{P}_{1,1,1,1,1}^4$	1	101	1	2
$\mathbb{P}_{3,3,1,1,1}^4$	4	112	2	4
$\mathbb{P}_{5,3,3,3,1}^4$	3	75	3	12
$\mathbb{P}_{5,5,5,4,1}^4$	5	65	5	56
$\mathbb{P}_{7,7,3,3,1}^4$	17	65	5	82
$\mathbb{P}_{6,6,3,2,1}^4$	7	79	5	100
$\mathbb{P}_{8,6,6,3,1}^4$	8	68	5	157
$\mathbb{P}_{8,8,4,3,1}^4$	10	70	6	296
$\mathbb{P}_{10,10,6,3,1}^4$	19	67	7	1709
$\mathbb{P}_{12,12,9,2,1}^4$	16	100	8	4854
$\mathbb{P}_{20,15,12,12,1}^4$	23	47	11	$\geq 703488$

---

<sup>4</sup>By a smooth phase we refer to those phases embedded in a smooth ambient toric variety

Manifold	$h_{toric}^{1,1}$	Phases	Smooth phases
$(4 5)$	1	2	1
$\left( \begin{array}{c c} 3 & 2 \ 2 \\ 2 & 2 \ 1 \end{array} \right)$	2	4	1
$\left( \begin{array}{c c} 4 & 2 \ 2 \ 1 \\ 1 & 0 \ 0 \ 2 \\ 1 & 1 \ 0 \ 1 \end{array} \right)$	3	6	1
$\left( \begin{array}{c c} 3 & 2 \ 1 \ 1 \ 0 \ 0 \ 0 \\ 3 & 0 \ 1 \ 0 \ 2 \ 1 \ 0 \\ 2 & 0 \ 0 \ 1 \ 0 \ 1 \ 1 \\ 1 & 0 \ 0 \ 0 \ 1 \ 0 \ 1 \end{array} \right)$	4	130	5
$\left( \begin{array}{c c} 2 & 1 \ 1 \ 1 \ 0 \ 0 \ 0 \ 0 \\ 2 & 1 \ 0 \ 0 \ 1 \ 1 \ 0 \ 0 \\ 2 & 0 \ 1 \ 0 \ 1 \ 0 \ 1 \ 0 \\ 2 & 0 \ 0 \ 1 \ 1 \ 0 \ 0 \ 1 \\ 2 & 0 \ 0 \ 0 \ 0 \ 1 \ 1 \ 1 \end{array} \right)$	5	22784	302
$\left( \begin{array}{c c} 2 & 1 \ 1 \ 1 \ 0 \ 0 \ 0 \ 0 \ 0 \\ 2 & 1 \ 0 \ 0 \ 1 \ 1 \ 0 \ 0 \ 0 \\ 2 & 0 \ 1 \ 0 \ 0 \ 0 \ 1 \ 1 \ 0 \\ 2 & 0 \ 0 \ 1 \ 0 \ 0 \ 0 \ 0 \ 1 \\ 2 & 0 \ 0 \ 0 \ 1 \ 0 \ 1 \ 0 \ 1 \\ 2 & 0 \ 0 \ 0 \ 0 \ 1 \ 0 \ 1 \ 0 \ 1 \end{array} \right)$	6	33415	33415
$\left( \begin{array}{c c} 2 & 1 \ 1 \ 1 \ 0 \ 0 \\ 1 & 1 \ 0 \ 0 \ 1 \ 0 \\ 1 & 0 \ 1 \ 0 \ 1 \ 0 \\ 1 & 0 \ 0 \ 1 \ 1 \ 0 \\ 1 & 1 \ 0 \ 0 \ 0 \ 1 \\ 1 & 0 \ 1 \ 0 \ 0 \ 1 \\ 1 & 0 \ 0 \ 1 \ 0 \ 1 \end{array} \right)$	7	22690	6168
$\left( \begin{array}{c c} 2 & 1 \ 1 \ 1 \ 0 \ 0 \ 0 \\ 1 & 1 \ 0 \ 0 \ 1 \ 0 \ 0 \\ 1 & 1 \ 0 \ 0 \ 0 \ 1 \ 0 \\ 1 & 0 \ 1 \ 0 \ 1 \ 0 \ 0 \\ 1 & 0 \ 0 \ 1 \ 0 \ 1 \ 0 \\ 1 & 0 \ 0 \ 0 \ 1 \ 0 \ 1 \\ 1 & 0 \ 0 \ 0 \ 0 \ 1 \ 1 \\ 1 & 0 \ 0 \ 0 \ 0 \ 0 \ 2 \end{array} \right)$	8	39772	6484

## 5. Special Examples of Phase Diagrams

Whereas in the previous examples, by our starting point we were guaranteed to have a Calabi-Yau sigma model region, here we note some examples which do not share this property. We will also see some examples in which there is no Landau-Ginzburg region, gauged or ungauged.

### Example 1

Consider the point set

$$\begin{aligned}
\alpha_1 &= (4, -3, 0, 0, 0, 0, 0, 0, 0) \\
\alpha_2 &= (0, 1, 0, 0, 0, 0, 0, 0, 0) \\
\alpha_3 &= (0, 0, 1, 0, 0, 0, 0, 0, 0) \\
\alpha_4 &= (0, 0, 0, 1, 0, 0, 0, 0, 0) \\
\alpha_5 &= (0, 0, 0, 0, 1, 0, 0, 0, 0) \\
\alpha_6 &= (0, 0, 0, 0, 0, 1, 0, 0, 0) \\
\alpha_7 &= (0, 0, 0, 0, 0, 0, 1, 0, 0) \\
\alpha_8 &= (-4, 2, -2, -1, -1, -2, -1, 4, -2) \\
\alpha_9 &= (0, 0, 0, 0, 0, 0, 0, 0, 1) \\
\alpha_{10} &= (3, -2, 0, 0, 0, 0, 0, 0, 0) \\
\alpha_{11} &= (2, -1, 0, 0, 0, 0, 0, 0, 0) \\
\alpha_{12} &= (1, 0, 0, 0, 0, 0, 0, 0, 0)
\end{aligned}$$

used in [4] to describe the toric variety  $\mathbb{C}^9/(\mathbb{Z}_4 \times \mathbb{Z}_4)$  whose  $h^{1,1} = 1$ . The 8 triangulations that occur here are easily described by noticing that  $\alpha_1, \alpha_2$  form a line with  $\alpha_{10}, \alpha_{11}, \alpha_{12}$  being points on it going from  $\alpha_1$  to  $\alpha_2$ . A triangulation of the cone corresponds to a choice of points among  $\alpha_{10}, \alpha_{11}, \alpha_{12}$  to include in the fan. If we don't include any of the 3 points, we obtain the original space  $\mathbb{C}^9/(\mathbb{Z}_4 \times \mathbb{Z}_4)$ , physically a LG model. Including all 3 points results in hybrid LG model based on a  $\mathbb{IP}_1$  vacuum. Other triangulations correspond to one of the above described phases. Notice that there is *not* a smooth Calabi-Yau sigma model phase for this theory. This means that in no phase can we properly interpret the (single) marginal operator whose charges qualify it for the role of a Kähler modulus as a geometrical radial mode. There is thus no “large radius limit” for this example – no limit in which classical geometrical reasoning can be used to describe the physical model.

### Example 2

In the last example we described a case where a potential Kähler form was present but no Calabi-Yau phase was to be found. Now we give an example where

there is no Kähler form and show how we can interpret this within the phases picture and indicate its implication for mirror symmetry.

We focus on the  $Z$ -manifold and its putative mirror. Recall that the  $Z$ -manifold has  $h^{1,1} = 36$  and  $h^{2,1} = 0$ , the latter implying that it is *rigid*. This seems to provide a puzzle for mirror symmetry as the putative mirror would have  $h^{1,1} = 0$  and hence would not be Kähler. Let analyze this in the context of the phases picture.

As discussed in [4] given the toric data for the  $Z$ -manifold, we can apply the mirror construction of [8] (as implemented by [7]) to yield the toric data for the mirror. This yields the pointset:

$$\begin{aligned}
\alpha_1 &= (3, 0, 0, 1, 1, 1, -1, -1, -3) \\
\alpha_2 &= (0, 1, 0, 0, 0, 0, 0, 0, 0) \\
\alpha_3 &= (0, 0, 1, 0, 0, 0, 0, 0, 0) \\
\alpha_4 &= (0, 0, 0, 1, 0, 0, 0, 0, 0) \\
\alpha_5 &= (0, 0, 0, 0, 1, 0, 0, 0, 0) \\
\alpha_6 &= (0, 0, 0, 0, 0, 1, 0, 0, 0) \\
\alpha_7 &= (0, 0, 0, 0, 0, 0, 1, 0, 0) \\
\alpha_8 &= (0, 0, 0, 0, 0, 0, 0, 1, 0) \\
\alpha_9 &= (0, -1, -1, -2, -2, -2, 0, 0, 3)
\end{aligned}$$

Given these points, we can now find all triangulations to yield the phase diagram. However, the above simplex of 9 points in 9 dimensions does not contain any interior points, thus there is only one triangulation, namely the simplex itself with volume 9. Mathematically, this corresponds to the toric variety  $\mathbb{C}^9/(\mathbb{Z}_3 \times \mathbb{Z}_3)$ . Physically, this is a Landau-Ginzburg theory. Thus, this enlarged Kähler moduli space consists of one-point, hence one phase, which by direct inspection is interpretable as a Landau-Ginzburg model. Quite consistently, there is no Calabi-Yau sigma model phase, as in the last example. Thus, there is no puzzle by the absence of a Kähler form since there is no geometrical phase in which it would be needed. Hence, in the generic Calabi-Yau example, the enlarged Kähler moduli spaces for both the manifold and its mirror contain smooth Calabi-Yau sigma model regions. Manifolds associated with these regions are called “mirror manifolds”. Mirror symmetry, though, is more general — and makes a one to one association between all points in the original moduli space with those in the mirror moduli space. In the degenerate case of a rigid Calabi-Yau manifold, the enlarged Kähler moduli space for its mirror is similarly degenerate: it lacks a Calabi-Yau sigma model region, precisely in keeping with the need to have  $h^{1,1} = 0$ . Thus, there is still a one to one association of theories, but none of these involve two Calabi-Yau manifolds.

In the context of the phases picture, therefore, the puzzle of identifying the mirror to a rigid Calabi-Yau manifold evaporates. This in no way precludes the possibility of there being some other geometrical interpretation, as has been proposed in [9] [10] [11]. It simply shows that such an interpretation is not necessary with our more robust understanding of conformal field theory moduli space.

**Example 3**

Now let's look at a  $h^{1,1} = 1$  example where we have no Landau-Ginzburg phase, and which also illustrates a rather special  $\mathbb{Z}_2$  symmetry relating the 2 phases. We consider here a complete intersection of 4 quadrics in  $\mathbb{P}^7$  giving rise to a Calabi-Yau manifold. The point set here is given by

$$\begin{aligned}
\alpha_1 &= (1, 0, 0, 0, 0, 0, 0, 1, 0, 0, 0) \\
\alpha_2 &= (0, 1, 0, 0, 0, 0, 0, 1, 0, 0, 0) \\
\alpha_3 &= (0, 0, 1, 0, 0, 0, 0, 0, 1, 0, 0) \\
\alpha_4 &= (0, 0, 0, 1, 0, 0, 0, 0, 1, 0, 0) \\
\alpha_5 &= (0, 0, 0, 0, 1, 0, 0, 0, 0, 1, 0) \\
\alpha_6 &= (0, 0, 0, 0, 0, 1, 0, 0, 0, 1, 0) \\
\alpha_7 &= (0, 0, 0, 0, 0, 0, 1, 0, 0, 0, 1) \\
\alpha_8 &= (-1, -1, -1, -1, -1, -1, -1, 0, 0, 0, 1) \\
\alpha_9 &= (0, 0, 0, 0, 0, 0, 0, 1, 0, 0, 0) \\
\alpha_{10} &= (0, 0, 0, 0, 0, 0, 0, 0, 1, 0, 0) \\
\alpha_{11} &= (0, 0, 0, 0, 0, 0, 0, 0, 0, 1, 0) \\
\alpha_{12} &= (0, 0, 0, 0, 0, 0, 0, 0, 0, 0, 1)
\end{aligned}$$

There are only two phases in this theory. One is the obvious Calabi-Yau phase given by the triangulation consisting of 8 simplices, where each simplex consists of  $\alpha_{10}, \alpha_{11}, \alpha_{12}$  and 8 points chosen from  $\alpha_1 \dots \alpha_9$ . Here the corresponding  $F_\Delta$  is  $(0, 0, 0, 0, 0, 0, 0) \times \mathbb{C}^4$ . The other phase corresponds to the symmetric operation of removing  $\mathbb{C}^7 \times (0, 0, 0, 0)$  and this results in a Landau-Ginzburg theory fibered over  $\mathbb{P}^3$ . The triangulation for this phase, as might be expected, consists of 4 simplices of volume 2, each given by  $\alpha_1 \dots \alpha_8$  and a choice of 3 points amongst  $\alpha_9 \dots \alpha_{12}$ . The  $\mathbb{Z}_2$  fibration over  $\mathbb{P}_3$  is easily understood from the charges of p-fields: When we divide the original  $S^8$  target space  $|p_1|^2 + |p_2|^2 + |p_3|^2 + |p_4|^2 = r$  by the  $U(1)$  to determine a representative in  $\mathbb{P}_3$ , the s-fields are identified up to a sign change due to the charges of the  $p$ 's. It's instructive to see how this comes about in the toric language. Consider any 2 simplices in the Calabi-Yau triangulation containing  $\alpha_9$  (associated with  $p_1$ ), say  $\{\alpha_1, \dots, \alpha_7, \alpha_9, \dots, \alpha_{12}\}$  (corresponding to the  $x_8 \neq 0$

patch in the  $\mathbb{P}^8$ ) and  $\{\alpha_1, \dots, \alpha_6, \alpha_8, \dots, \alpha_{12}\}$  (corresponding to  $x_7 \neq 0$ ), each of which has volume 1. We now partially star unsubdivide on the  $\alpha_9$  (i.e. remove  $\alpha_9$  from both simplices and form a resulting simplex as a union of the remaining subsimplices), giving a nonzero expectation value to  $p_1$  and obtaining a volume 2 resultant simplex formed by the blowing down of a  $\mathbb{P}^1$  ( $x_7 \neq 0$  or  $x_8 \neq 0$ ). Thus we have collapsed 2 patches of  $\mathbb{P}^8$  (whose union is the whole of  $\mathbb{P}^8$ ) into a singular point over a  $\mathbb{P}^3$  patch ( $p_1 \neq 0, p_2 \dots p_4$  arbitrary). By doing similar unsubdivisions for the other simplices we obtain a  $\mathbb{C}^8/\mathbb{Z}_2$  fiber over a  $\mathbb{P}_3$  as expected.

An important observation, originally made in [12] is that the mirror to this manifold, which has  $h^{2,1} = 1$ , admits a  $\mathbb{Z}_2$  symmetry on its complex structure moduli space. Reinterpreted back on the original manifold being studied here this identifies the two phases just discussed [4]. Thus, the ‘‘small’’ radius phase, involving a Landau-Ginzburg fibration on a  $\mathbb{P}^3$ , can be reinterpreted as a large radius Calabi-Yau sigma model. This gives an unambiguous  $R \rightarrow 1/R$  type symmetry in the Calabi-Yau context.

**Example 4**

We now come to an example where all phase regions turn out to be Calabi-Yau. Let’s in particular consider the following example, which will also contain a rather explicit symmetry relating the 4 phase regions.

$$\left( \begin{array}{c|ccc} 2 & 1 & 1 & 1 \\ 2 & 1 & 1 & 1 \\ 2 & 1 & 1 & 1 \end{array} \right) \tag{17}$$

The point set here is

- $\alpha_1 = (1, 0, 0, 0, 0, 0, 1, 0, 0)$
- $\alpha_2 = (0, 1, 0, 0, 0, 0, 0, 1, 0)$
- $\alpha_3 = (-1, -1, 0, 0, 0, 0, 0, 0, 1)$
- $\alpha_4 = (0, 0, 1, 0, 0, 0, 1, 0, 0)$
- $\alpha_5 = (0, 0, 0, 1, 0, 0, 0, 1, 0)$
- $\alpha_6 = (0, 0, -1, -1, 0, 0, 0, 0, 1)$
- $\alpha_7 = (0, 0, 0, 0, 1, 0, 1, 0, 0)$
- $\alpha_8 = (0, 0, 0, 0, 0, 1, 0, 1, 0)$
- $\alpha_9 = (0, 0, 0, 0, -1, -1, 0, 0, 1)$
- $\alpha_{10} = (0, 0, 0, 0, 0, 0, 1, 0, 0)$
- $\alpha_{11} = (0, 0, 0, 0, 0, 0, 0, 1, 0)$
- $\alpha_{12} = (0, 0, 0, 0, 0, 0, 0, 0, 1)$

There are only 4 triangulations of the above set of points, and they are easily identified by the set of points that belong to every simplex. The original Calabi-Yau has  $\{\alpha_{10}, \alpha_{11}, \alpha_{12}\}$  in each of its simplices. The other triangulations are obtained from permuting this set. The superpotential here is nicely symmetric in each set of variables. The D-term appears to treat the  $\phi$  and  $p$ -fields asymmetrically, however, the importance of this asymmetry is only to determine which fields will span the direct sum of line bundles over the product of  $\mathbb{P}^2$ 's in which the Calabi-Yau is embedded. The symmetry we are referring to is linked to the choice of representation of the asymmetry, i.e. to the choice of fields spanning the line bundles. To see this explicitly, we note that minimization of the D-term requires  $\sum_{i=1}^3 |p_i|^2 = \sum_{i=1}^3 |\phi_i|^2 - r_1$ . This allows us to substitute for the sum of the  $p_i$ 's in the other two parts of the D-term with  $\phi_1, \phi_2, \phi_3$ , leading to a D-term which has  $\phi_1, \phi_2, \phi_3$  as  $p$ -fields and 3 independent  $r$ -parameters  $-r_1, r_2 - r_1, r_3 - r_1$ . Thus, all four phases are smooth CY and are actually isomorphic.

## 6. Conclusions

The moduli space of  $N = 2$  superconformal field theories contains within it a surprising wealth of both physical and geometrical content. We have seen that the phase diagram of those theories smoothly connected to one another by truly marginal deformations decomposes into numerous phases. Within each phase there is a region for which perturbative methods are reliable provided one expands around an appropriate description of the physical model. The identity of such a model is thereby naturally associated with each region.

Some time ago it was shown that there are examples which have regions corresponding to Calabi-Yau sigma models on topologically distinct target spaces. Nonetheless, the physical model can smoothly interpolate from one region to any other and hence the target space topology can change without a physical discontinuity. We described some further properties of these phase diagrams in this talk and found some other interesting features. We have seen that the sheer number of phase regions grows quite quickly with the number of moduli parameters. The “typical” such phase diagram has regions identifiable as smooth Calabi-Yau sigma models, orbifold Calabi-Yau sigma models, Landau-Ginzburg, and hybrid combinations thereof. We have emphasized, though, that there are other examples in which some of these typical types of models do not arise. For instance, we have seen examples where there is no variety of Landau-Ginzburg theory – all regions having a Calabi-Yau like interpretation. We have seen other examples that give us the first unambiguous  $R \rightarrow 1/R$  symmetry. And finally, we have seen examples which have no variety of Calabi-Yau sigma model interpretation. The latter have

provided us with a satisfying perspective on what it means to have mirror symmetry in the context of rigid Calabi-Yau manifolds.

An interesting and important area to pursue is the application of all of this formalism to the setting of  $(0, 2)$  models. Such work is in progress and will be reported upon shortly.

## References

- [1] E. Witten, *Phases of  $N=2$  Theories in Two Dimensions*, Nucl. Phys. **B403** (1993) 159.
- [2] P. Aspinwall, B. Greene, and D. Morrison, *Calabi-Yau Moduli Space, Mirror Manifolds, and Spacetime Topology Change in String Theory*, Nucl. Phys. **B416** (1994) 414.
- [3] B. Greene, C. Vafa and N. Warner, *Calabi-Yau Manifolds and Renormalization Group Flows*, Nucl. Phys. **B324** (1989) 371.
- [4] P. Aspinwall and B. Greene, *On the Geometric Interpretation of  $N = 2$  Superconformal Theories*, hep-th/9409110
- [5] A. Strominger, *Massless Black Holes and Conifolds in String Theory*, hep-th/9504090
- [6] B. R. Greene, D. R. Morrison, and A. Strominger, *Black Hole Condensation and the Unification of String Vacua*, hep-th/9504145
- [7] V. Batyrev, *Dual Polyhedra and Mirror Symmetry for Calabi-Yau Hypersurfaces in Toric Varieties*, J. Alg. Geom. **3** (1994) 493-535.
- [8] B. R. Greene and M. R. Plesser, *Duality in Calabi-Yau Moduli Space*, Nucl. Phys. **B338** (1990) 15-37
- [9] P. Candelas, E. Derrick and L. Parkes, *Generalized Calabi-Yau Manifolds and the Mirror of a Rigid Manifold*, Nucl. Phys. **B407** (1993) 115.
- [10] R. Schimmrigk, *Critical Superstring Vacua from Noncritical Manifolds: A Novel Framework for String Compactification*, Phys. Rev. Lett. **70** (1993) 3688.
- [11] S. Sethi, *Supermanifolds, Rigid Manifolds and Mirror Symmetry*, Harvard 1994 preprint HUTP-94-A002, hep-th/9404186
- [12] P. Berglund, P. Candelas, X. de la Ossa, A. Font, T. Hubsch, D. Jančić and F. Quevedo, *Periods for Calabi-Yau and Landau-Ginzburg Vacua*, hep-th/9308005